Chemistry & Biology, Vol. 12, 973–980, September, 2005, ©2005 Elsevier Ltd All rights reserved. DOI 10.1016/j.chembiol.2005.07.009

Methylxanthine Drugs Are Chitinase Inhibitors: Investigation of Inhibition and Binding Modes

Brief Communication

Francesco V. Rao,[1] Ole A. Andersen,[1] Kalpit A. Vora,[2] Julie A. DeMartino,[2] and Daan M.F. van Aalten[1,*]

[1]Division of Biological Chemistry and Molecular Microbiology
School of Life Sciences
University of Dundee
Dundee DD1 5EH
Scotland

[2]Department of Immunology
Merck Research Laboratories
Rahway, New Jersey 07065

Summary

Family 18 chitinases play key roles in a range of pathogenic organisms and are overexpressed in the asthmatic lung. By screening a library of marketed drug molecules, we have identified methylxanthine derivatives as possible inhibitor leads. These derivatives, theophylline, caffeine, and pentoxifylline, are used therapeutically as antiinflammatory agents, with pleiotropic mechanisms of action. Here it is shown that they are also competitive inhibitors against a fungal family 18 chitinase, with pentoxifylline being the most potent (K_i of 37 μM). Crystallographic analysis of chitinase-inhibitor complexes revealed specific interactions with the active site, mimicking the reaction intermediate analog, allosamidin. Mutagenesis identified the key active site residues, conserved in mammalian chitinases, which contribute to inhibitor affinity. Enzyme assays also revealed that these methylxanthines are active against human chitinases.

Introduction

Chitin, a polymer of β(1,4)-linked *N*-acetylglucosamine (GlcNAc), is an essential structural component of fungal cell walls, the shells of nematode eggs, and arthropod exoskeletons. Family 18 chitinases (CAZY GH 18 [1]), which degrade this polymer, play key roles in the life cycles of pathogenic fungi [2–4], nematodes [5], malaria [6, 7], and insects [8–11]. In addition, a recent study has shown that inhibition of a mammalian chitinase associated with parasitic infections reduces recruitment of inflammatory cells and profoundly dampens T helper 2 (Th2) cellular responses in a murine model of lung inflammation, suggesting that this enzyme may be a potential target for an asthma drug therapy [12]. The enzymes have a conserved $(\beta/\alpha)_8$ fold, with a surface groove containing exposed aromatic residues, used for binding the chitin substrate [13–18]. Family 18 chitinases employ an unusual reaction mechanism, in which the acid protonating the glycosidic bond is a conserved glutamate and the nucleophile is the oxygen of the *N*-acetyl group on the –1 sugar (the sugar on the nonreducing end of the glycosidic bond), forming an oxazolinium ion intermediate [13, 15, 19]. A range of chitinase inhibitors has been described, most of which are natural products. Allosamidin is a pseudotrisaccharide that mimics the oxazolinium reaction intermediate, inhibiting family 18 chitinases in the nanomolar-micromolar range [4, 8, 13, 15, 18, 20, 21]. Argifin, argadin, and CI-4 are peptide-based inhibitors that mimic protein-carbohydrate interactions, both in terms of hydrogen bonds and stacking interactions [10, 11, 18, 22–25]. Unfortunately, all currently available inhibitors have a number of properties that make them unsuitable as inhibitor leads, including high molecular weights (e.g., allosamidin, argifin, argadin), several stereocenters, and low cLogP values (e.g., –5.2 for allosamidin). More importantly, there is only limited availability of family 18 chitinase inhibitors with an $IC_{50} < 0.5$ mM, hampering further inhibition studies of these enzymes.

To aid the development of potent, drug-like, and readily available chitinase inhibitors, we have screened a drug library, leading to the identification of methylxanthines as a potential scaffold. The drugs theophylline, caffeine, and pentoxifylline, which contain the 1,3-dimethylxanthine substructure, were studied in terms of their inhibition and structural mode of binding against a family 18 chitinase from the opportunistic fungal pathogen *Aspergillus fumigatus*, showing that pentoxifylline inhibits with a K_i of 37 μM by forming extensive π-π stacking interactions with conserved tryptophans in the active site of this protein. The activity of mammalian chitinases, containing homologous active site amino acid residues in their primary amino acid sequences, are likewise inhibited by these xanthine derivatives.

Results

Inhibitor Screening

A commercially available library of 880 drug molecules was screened at 100 μM against a family 18 chitinase, chitinase B1 from *A. fumigatus* (AfChiB1), using a fluorescent assay (Figure 1A). After elimination of apparent false positives (specifically, the hits in the far lower left corner of Figure 1A), two methylxanthine derivatives, theophylline and pentoxifylline, were identified, possessing a common 1,3-dimethylxanthine substructure, which were the subject of further analyses. Inhibition by theophylline and pentoxifylline, and the closely related methylxanthine caffeine, was initially confirmed by dose-response curves (Figure 1B), with IC_{50}s ranging from 1500 μM (theophylline) to 126 μM (pentoxifylline), as presented in Table 1. Initial enzyme velocity measurements at different concentrations of substrate (5–30 μM) and pentoxifylline (0, 60, 50, and 200 μM) were used to demonstrate that pentoxifylline is a competitive inhibitor, with a K_i of 37 μM (Figure 1C and Table 1).

Humans possess two family 18 chitinases, a chitotriosidase (hCHT) [26] and acidic mammalian chitinase

*Correspondence: dava@davapc1.bioch.dundee.ac.uk

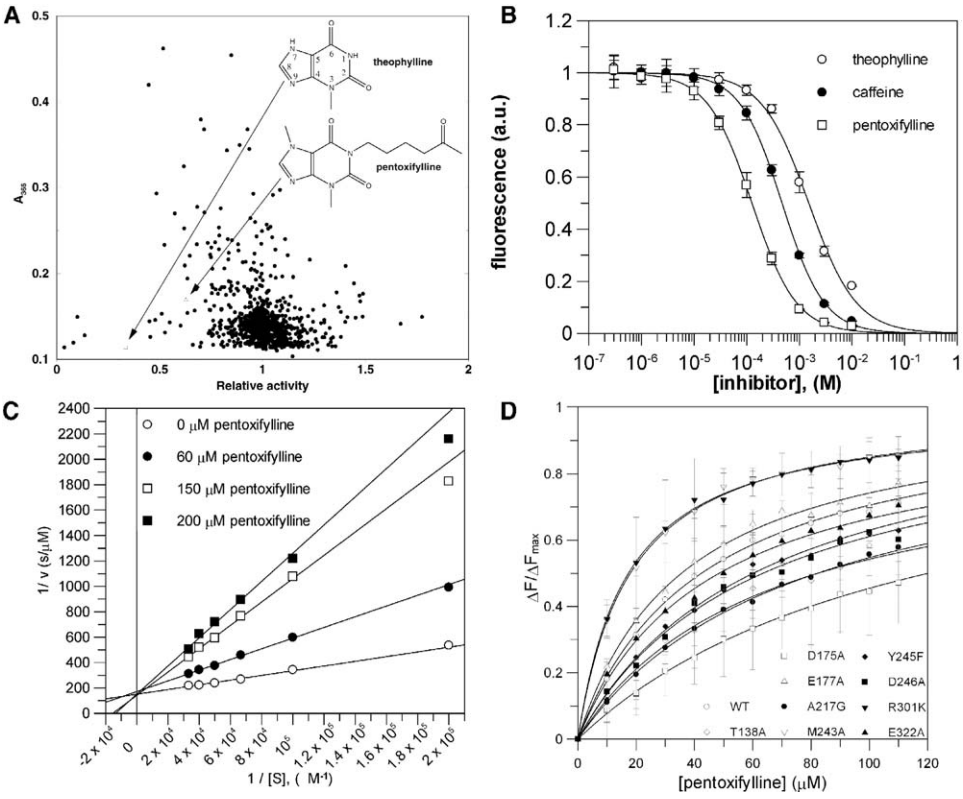

Figure 1. Characterization of Theophylline, Caffeine, and Pentoxifylline Inhibition

(A) Results of the library screen, showing percentage remaining activity as measured by liberated 4-methylumbelliferone (horizontal axis) versus absorbance measured at 360 nm (vertical axis), resulting from intrinsic absorbance at the excitation wavelength used for the fluorescence measurement. Hits in the lower left corner thus indicate compounds that do not themselves absorb at the excitation wavelength, yet do show reduced fluorescence and, thus, reduced activity. Two hits, aminophylline (containing theophylline as active ingredient) and pentoxifylline are indicated, together with their chemical structures.

(B) Dose-response curves for the methylxanthine inhibitors measured against AfChiB1.

(C) Lineweaver-Burk plots of pentoxifylline measured against AfChiB1 at different concentrations of the inhibitor. A fit of all the data against a competitive inhibition model resulted in a K_i of 37 ± 2 μM, with a V_{max} of 0.0072 ± 0.0002 μM/s and a K_m of 12.9 ± 0.9 μM.

(D) Tryptophan fluorescence binding experiments of pentoxifylline against wild-type and mutant AfChiB1. The data points, fluorescence with λ_{ex}=295 nm and λ_{em}=345 nm, were corrected for inner filter effects (due to absorbance of the xanthine at λ_{ex}) using $F_{corr} = F_{obs} \cdot 10^{(0.5 \cdot A)}$, where A is the pentoxifylline absorbance at 295 nm. The data were then fitted with GraFit [49] to a single-site binding equation $\Delta F/\Delta F_{max} = (C \cdot [L])/(K_d + [L])$, where C is the capacity and [L] is the ligand concentration. Experiments were performed in triplicate, except for the D175A, E177A, and Y245F mutants, which were in duplicate.

(AMCase), an enzyme with an unusual acidic pH optimum [27], the in vivo elaboration of which is probably evolutionarily tied to protective antiparasitic host responses to chitin-bearing pathogens. These enzymes, like AfChiB1, are of the "bacterial" type of family 18 chitinases, possessing a deep catalytic cleft lined with solvent-exposed aromatic residues [17], sharing 31% and 28% sequence identity with AfChiB1, respectively. Accordingly, the methylxanthines also inhibit the human chitinases, with IC_{50}s up to 98 μM, for pentoxifylline (Table 1).

Among their pleiotropic mechanisms of action, methylxanthine derivatives have also variously been reported as phosphodiesterase inhibitors [28, 29], adenosine receptor antagonists [30], and inducers of histone deacetylase (HDAC) activity [31]. The inhibition of human phosphodiesterase-4 by theophylline, caffeine, and pentoxifylline was measured using a PDE-SPA assay, and IC_{50}s were determined to be in the high μM range (Table 1), consistent with potencies published elsewhere [32]. As a further control, inhibitory potential of these xanthine derivatives was tested against two other glycoside hydrolases, lysozyme (using a fluorescein-based assay) and cellulase from *Aspergillus niger* (CAZY family GH 8 [1]), using a fluorescent substrate, showing, at most, approximately 1 mM inhibition for cellulase and none for lysozyme (Table 1). Similarly, allosamidin is known to not inhibit lysozyme [33]. Together these data suggest that there may be a specific AfChiB1-pentoxifylline interaction, prompting us to investigate the precise binding mode.

Structure of Chitinase-Inhibitor Complexes

To determine the mode of binding of theophylline, caffeine, and pentoxifylline to the fungal chitinase, AfChiB1 crystals were soaked with the inhibitors, followed by collection of X-ray diffraction data (Table 2). In addition, a similar procedure was used to obtain a

Table 1. Methylxanthine Inhibition/Binding of Family 18 Chitinases, a Phosphodiesterase, and Two Control Glycoside Hydrolases

	Theophylline	Caffeine	Pentoxifylline
AfChiB1 IC_{50} (μM)	1500 ± 90	469 ± 23	126 ± 7 (K_i = 37 ± 2)
AfChiB1 K_d (μM)	—	—	43 ± 10
AfChiB1-A217G K_d (μM)	—	—	77 ± 9
AfChiB1-D175A K_d (μM)	—	—	100 ± 8
AfChiB1-D246A K_d (μM)	—	—	62 ± 23
AfChiB1-E322A K_d (μM)	—	—	45 ± 9
AfChiB1-M243A K_d (μM)	—	—	18 ± 1
AfChiB1-E177A K_d (μM)	—	—	36 ± 7
AfChiB1-R301K K_d (μM)	—	—	17 ± 3
AfChiB1-W137A K_d (μM)	—	—	n.d.[a]
AfChiB1-T138A K_d (μM)	—	—	65 ± 34
AfChiB1-Y245F K_d (μM)	—	—	64 ± 20
hCHT IC_{50} (μM)	>500	257 ± 8	98 ± 8
hAMCase activity at 1 mM (%)	36	36	49
Aspergillus niger cellulase IC_{50} (μM)	1008 ± 159	1250 ± 278	881 ± 319
Egg white lysozyme activity at 500 μM (%)	100	100	100
hPDE-4 IC_{50} (μM)	386 ± 39	747 ± 212	168 ± 105

IC_{50}s were determined as discussed in the text, and as shown for AfChiB1 in Figure 1B. The pentoxifylline K_i was determined by fitting all data shown in Figure 1C to the standard equation for a competitive inhibitor (see legend to Figure 1C). The K_ds were determined from tryptophan fluorescence binding experiments, as shown and explained in Figure 1D.
[a] n.d. indicates that there was no detectable binding.

complex of the well-known chitinase inhibitor allosamidin [8] with AfChiB1. Allosamidin has been cocrystallized with a range of chitinases and the mode of inhibition described in great detail [13, 20, 21, 34, 35]—the structure is used here for comparison purposes only. The methylxanthine-AfChiB1 complexes were refined against high-resolution X-ray diffraction data (Table 2), with the inhibitors well defined by unbiased $|F_o| - |F_c|$, ϕ_{calc} electron density maps (Figure 2). All three inhibitors show the same surprising mode of binding, with a common position for the methylxanthine substructure (equivalent to theophylline). In the complex of AfChiB1 with theophylline, the weakest of the three inhibitors, with an IC_{50} of 1500 μM, the inhibitor binds in a position equivalent to the allosamidin allosamizoline moiety (Figure 2), termed the –1 position, as it is equivalent to the GlcNAc subsite on the nonreducing end of the glycosidic bond [13, 15, 36, 37]. This allosamizoline moiety is known to mimic the oxazolinium ion reaction intermediate formed upon nucleophilic attack of the *N*-acetyl oxygen on the anomeric carbon [15, 19]. The methylxanthine core not only structurally mimics this intermediate, but also makes similar interactions with the chitinase. The xanthine ring appears to make favorable π-π stacking interactions with Trp385 (40 $Å^2$ total buried inhibitor surface), which is conserved in all active family 18 chitinases, and also interacts with the allosamizoline moiety in the allosamidin complex (Figure 2). Hydrogen bonds are formed with Asp175, Tyr245, and the backbone nitrogen of Trp137, residues all conserved in family 18 chitinases. Further water-mediated hydrogen bonds are observed from the O2 oxygen to Asp246 and Arg301. In addition to the methylxanthine in the –1 subsite, an additional ordered

Table 2. Details of Data Collection and Structure Refinement

	Theophylline	Caffeine	Pentoxifylline	Allosamidin
Resolution range (Å)	20–2.1 (2.17–2.1)	20–1.90 (1.97–1.90)	25–2.0 (2.07–2.0)	20–1.95 (2.02–1.95)
No. of Observed reflections	336,712 (30,248)	371,358 (34,086)	235,428 (19,469)	289,598 (27,689)
No. of Unique reflections	78,640 (7,728)	105,887 (10,440)	86,043 (7,767)	98782 (9,816)
Redundancy	4.3 (3.9)	3.5 (3.3)	2.7 (2.5)	2.9 (2.8)
I/σI	8.4 (2.6)	16.9 (4.2)	15.6 (2.6)	13.1 (2.2)
Completeness (%)	99.5 (98.0)	99.7 (98.9)	94.2 (85.5)	99.8 (99.7)
R_{merge}	0.136 (0.540)	0.043 (0.301)	0.049 (0.384)	0.063 (0.563)
R_{cryst}, R_{free}	0.185, 0.225	0.176, 0.202	0.187, 0.219	0.195, 0.224
Rmsd from ideal geometry				
Bonds (Å)	0.01	0.01	0.008	0.007
Angles (°)	1.5	1.4	1.5	1.4
B factor rmsd ($Å^2$)				
Bonded, main chain	1.6	1.5	1.4	1.5
<B> protein[a]	28.2	24.2	27.4	28.7
<B> ligand[a]	45.6	35.9	36.9	22.2
<B> water[a]	36.5	35.7	36.2	37.8

Values in parentheses are for the highest resolution shell. Crystals were of space group $P4_1$ and were cryo-cooled to 100 K. All measured data were included in structure refinement.
[a] <B> = average B factor.

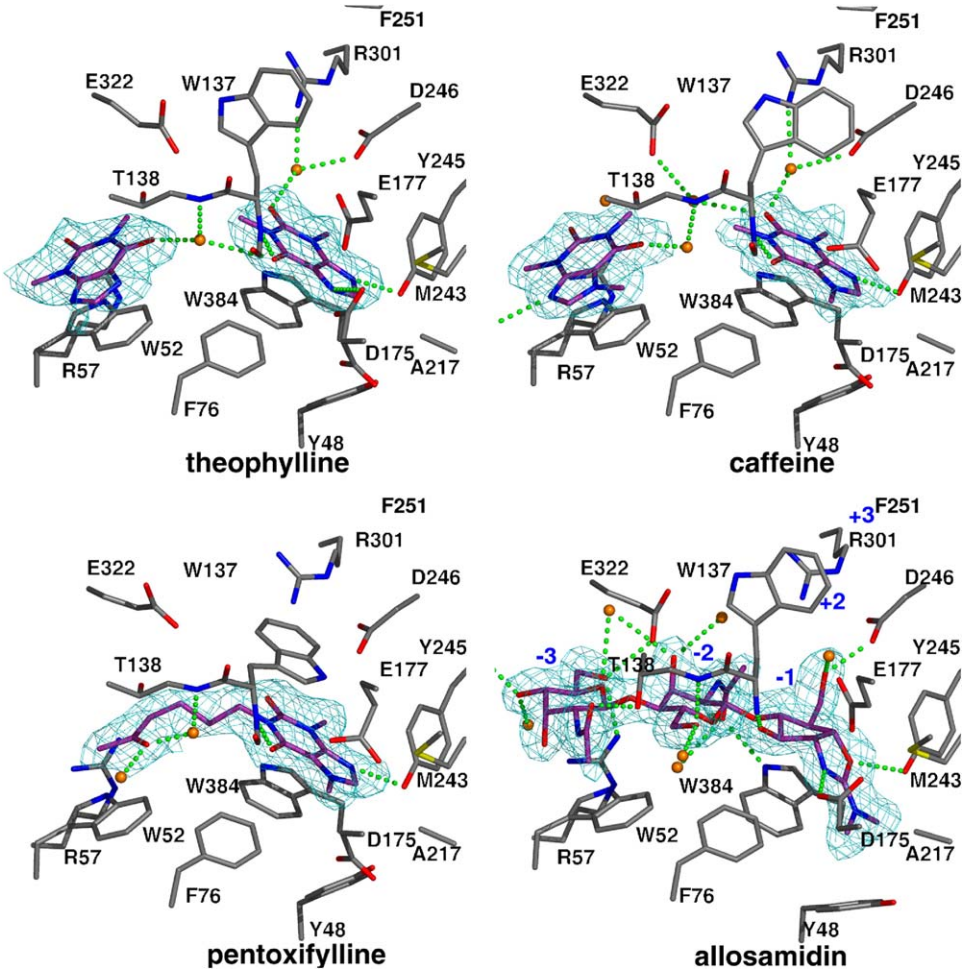

Figure 2. Structures of the AfChiB1 Inhibitor Complexes

AfChiB1 residues lining the active site are shown as sticks with gray carbon atoms. Inhibitor molecules are shown as sticks with magenta carbon atoms. Protein-inhibitor hydrogen bonds, calculated with PRODRG [48] and WHAT IF [52], are shown as dotted green lines. Unbiased (i.e., before inclusion of any inhibitor model) $|F_o| - |F_c|$, ϕ_{calc} electron density maps are shown at 2.5 σ. In the allosamidin complex, the sugar subsites are labeled in blue from –3 to –1; the approximate positions of the +1 and +2 subsites are also shown.

inhibitor molecule is observed occupying a position equivalent to the –3 sugar in the allosamidin complex (Figure 2). This additional methylxanthine molecule also makes stacking interactions with a tryptophan (Trp52), which is conserved in the other "bacterial"-type chitinases (e.g., the human chitotriosidase [17], AMCase [27], and chitinase A from *Serratia marcescens* [14, 37]).

Compared to theophylline, caffeine contains an additional 7-methyl group, which appears to increase inhibition 3-fold to an IC_{50} of 469 μM. In the AfChiB1 complex (Figure 2), caffeine binds identically to theophylline. This is surprising, as the addition of a 7-methyl group not only results in loss of the hydrogen bond for the xanthine-N7 with Asp175, but also forces Asp175 in the "down" conformation, compared to the "up" conformation in the allosamidin complex (Figure 2). Similarly, Glu177 moves away to avoid steric clashes of the terminal carboxylate with the N7-methyl. Again, an additional ordered inhibitor molecule is observed in the –3 subsite.

Pentoxifylline is the most potent of the three methylxanthine inhibitors against the fungal chitinase, with a K_i of 37 μM (Table 1). The AfChiB1-pentoxifylline complex reveals several additional interactions, which may explain the order of magnitude increase in potency compared to caffeine (Figure 2). Strikingly, Trp137 rotates 93° around χ_1, sandwiching the xanthine moiety with extensive π-π stacking interactions (approximately 25 Å^2 additional buried surface). The rotation of Trp137 excludes an ordered water molecule seen in the theophylline and caffeine complexes (Figure 2). Furthermore, the pentoxifylline alkyl-aldehyde tail extends into the –3 subsite, replacing the second ordered xanthine seen in both the theophylline and caffeine complexes, stacking with Trp52 and hydrogen bonding two ordered water molecules (Figure 2).

To probe the contributions of individual residues in the active site to pentoxifylline binding, interactions between mutant forms of AfChiB1 and the inhibitor were measured with tryptophan fluorescence, exploiting the

large conformational change of Trp137 (Table 1 and Figure 1D). The K_d for pentoxifylline with the wild-type enzyme was determined to be 43 ± 10 μM, which is in good agreement with the K_i (37 ± 2 μM) measured from the kinetics experiment. Surprisingly, none of the mutants show greater than 2.5-fold effects on binding, with the exception of the Trp137Ala mutant, which abrogates the detectable fluorescence quenching signal. The two mutants that most increase affinity (about 2-fold) are Met243Ala and Arg301Lys. Interestingly, Met243 sterically clashes with the inhibitor, with the shortest distance being 3.2 Å (between pentoxifylline-N8 and Met243-Sδ—the hydrogen atom on pentoxifylline-N8 would approach Met243-Sδ even closer), and mutation to alanine relieves this clash (Figure 2). In allosamidin, this unfavorable interaction with Met243 does not exist due to the "kink" between the two five-membered rings, whereas the pentoxifylline purine is flat (Figure 2). Similarly, the Arg301Lys mutant may increase binding as the flipped Trp137 indole ring closely approaches the Arg301 guanidinium group (shortest distance, 3.8 Å from Trp137-Cη2 to Arg301-Nη2; Figure 2). The two mutants that most decrease affinity (about 2-fold) are Asp175Ala and Ala217Gly. Ala217 forms the bottom of the pocket for the methyls on allosamidin's allosamizoline moiety; mutation to an alanine could lead to a large unoccupied pocket below the pentoxifylline purine ring. Similarly, mutation of Asp175 to Ala would cause the purine ring to bury the unsatisfied hydrogen bond donor Tyr48 (Figure 2). Strikingly, the Y245F mutation, which removes the only direct side-chain inhibitor hydrogen bond observed in the complex, only reduces the affinity 1.5-fold (Figure 2, Table 1).

Discussion

Using a screening approach, several methylxanthines were identified that inhibit family 18 chitinases, the most potent being pentoxifylline, showing a K_i of up to 37 μM against the chitinase AfChiB1 from the fungal pathogen *A. fumigatus*. These molecules are small and drug-like and make extensive hydrogen bonding and π-π stacking interactions with the active site, which appear to be unique to the chitinase, as the other glycosidases tested show only poor inhibition. The largest of these inhibitors, pentoxifylline, only covers a small part of the AfChiB1 active site, from the −1 to just beyond the −2 subsite. By comparison, other more potent chitinase inhibitors, such as allosamidin (which covers the −1 to −3 subsites, Figure 2) and argifin/argadin (which cover the −1 to +2 subsites [18, 23]) occupy further subsites. It should be noted that nearly all residues in the −1 subsite are identical in the "bacterial"- and "plant"-types of chitinases [35], suggesting these inhibitors may also reduce activity of the latter class of enzymes.

Previous analyses of the binding mode of methylxanthines in the phosphodiesterases show that the N1-methyl projects into a small pocket, suggesting that there is no additional space to derivatize much beyond the pentoxifylline side chain [38, 39]. Thus, it should be possible to extend the methylxanthine scaffold to address the additional available chitinase subsites and increase chitinase affinity and selectivity through synthetically accessible purine chemistry. Molecules of this nature may help elucidate the role that chitinases play in fungal morphology, growth, and virulence. Similarly, this approach may extend to the study of the precise functions of the mammalian chitinases. In this regard, chitotriosidase and acidic mammalian chitinase, as well as several structurally related, more family 18 chitinase-like lectins (chilectins), purported to be involved in carbohydrate recognition, such as HCgp-39, YM-1, and YM-2, have been implicated in the pathophysiology of inflammation (reviewed in [40]). Chitotriosidase is expressed in activated macrophages, and its levels are known to be upregulated both in atherosclerosis and in patients with Gaucher's lipid storage disease [26]. Acidic mammalian chitinase expression has been shown to be upregulated in the lungs of asthmatics, as well as in mice that develop airway hyperresponsiveness following antigen sensitization and challenge [12]. In the latter instance, inhibitors of AMCase (neutralizing antisera, allosamidin) efficaciously decreased airway hyperresponsiveness, reduced inflammatory cell influx into bronchiolar alveolar lavage fluid, and ameliorated airway inflammation. Anti-inflammatory effects of methylxanthine derivatives in vivo have already been well documented. For instance, theophylline has a greater than 50-year history as an asthma drug and acts not only as a bronchodilator, but also as an immunomodulator that downregulates the function of inflammatory cells in vitro and in vivo (reviewed in [41]). Pentoxifylline, a drug used clinically to treat peripheral vascular disease, likewise has immune-modulating properties [42, 43], including the ability to suppress inflammatory cytokine production. This drug has also been demonstrated to blunt airway hyperresponsiveness during allergen sensitization in rodent models of allergic inflammation [44]. The proposed mechanisms of action for theophylline and pentoxifylline action thought to occur at clinically relevant drug concentrations are nonspecific phosphodiesterase isozyme inhibition and nonselective antagonism of adenosine receptors [28–30]. Future research could investigate whether the methylxanthine derivatives identified here affect chitinase activity in an anti-asthma setting.

Significance

Family 18 chitinases play key roles in a range of chitin-containing pathogenic organisms and are overexpressed in the asthmatic lung. So far, no drug-like inhibitors for this family of enzymes have been described. This article reports the results of a screen against a library of drug molecules, identifying the methylxanthine drugs theophylline, caffeine, and pentoxifylline as micromolar inhibitors. These molecules show an unexpected binding mode involving extensive stacking interactions, and provide attractive, synthetically accessible scaffolds for further optimization.

Experimental Procedures

Purification, Crystallization, and Structure Determination

AfChiB1 was expressed, purified, and crystallized as previously described [18]. Briefly, AfChiB1 was overexpressed as a GST-fusion

protein in *Escherichia coli* and purified using a combination of affinity and size-exclusion chromatography. Pure AfChiB1 protein in 50 mM TRIS/HCl (pH 8) was spin-concentrated to 28 mg/ml. Vapor diffusion crystallization experiments were set up by mixing 1 μl of protein and 1 μl of mother liquor, consisting of 0.1 M Tris/HCl (pH 9.5) and 1.4 M Li_2SO_4, and equilibrated against a reservoir containing 0.5 ml of mother liquor. Crystals used for soaking experiments were washed three times in 0.1 M sodium citrate (pH 5.5) and 1.4 M Li_2SO_4, and thereafter soaked in mother liquor containing 3.8, 3.8, 20.0, and 9.0 mM ligand, with soaking times of 20, 5, 10, and 30 min for the theophylline, caffeine, pentoxifylline, and allosamidin inhibitors, respectively. The crystals were cryoprotected by a 10 s immersion in 3 M Li_2SO_4 and frozen in a nitrogen cryostream for data collection. Data were collected on a rotating anode and processed with the HKL suite of programs [45].

Refinement of the AfChiB1-inhibitor complexes was performed with CNS [46] interspersed with model building in O [47], starting from the native AfChiB structure (PDB entry 1W9P [18]). Models for the ligands were not included until their conformations were well defined by the unbiased $|F_o| - |F_c|$, ϕ_{calc} electron density maps (Figure 2). Due to the relatively high inhibitor concentrations used for soaking, electron density for additional, less ordered inhibitor molecules appear out with the –1 subsite. In the interest of simplicity, differences between the complexes are discussed using the first AfChiB monomer in the coordinate files, and analysis of inhibitor binding is focused on the active site only. Topologies for the ligands were obtained from the PRODRG server [48]. Images were generated with PyMol (available online at: http://www.pymol.org).

AfChiB1 Enzymology and Mutagenesis

AfChiB1 inhibition was studied using the fluorogenic substrate 4-methylumbelliferyl-β-D-*N*,*N*′-diacetylchitobiose (4MU-$GlcNAc_2$; Sigma Chemical, St. Louis, MO), following hydrolysis measuring liberated, fluorescent 4-methylumbelliferone (4MU), as described previously [18]. Briefly, in a final volume of 50 μl, 2 nM of enzyme was incubated with 20 μM substrate in McIlvain buffer (100 mM citric acid, 200 mM sodium phosphate [pH 5.5]) containing 0.1 mg/ml BSA, for 10 min at 37°C in the presence of different concentration of inhibitors. After the addition of 25 μl of 3 M glycine-NaOH (pH 10.3), the fluorescence of the liberated 4MU was quantified using a Flx 800 microtiterplate fluorescence reader (Bio-Tek Instruments), with excitation and emission wavelengths of 360 nm and 460 nm, respectively, using 40 nm slits. Experiments were performed in triplicate. Production of 4MU was linear with time for the incubation period used, and less than 10% of available substrate was hydrolyzed.

AfChiB1 was screened against a small molecule library of 880 compounds (Prestwick Chemical, France). The library was screened with 50 μl assay volumes in 96-well plates using 2 nM of enzyme, 0.1 mg/ml BSA, and 20 μM substrate and 100 μM inhibitor, assuming a compound molecular weight of 500 Da. To remove false positives of compounds that absorb at the excitation wavelength used for measuring 4MU concentration (and thus enzyme activity), absorbance at the excitation wavelength (360 nm) was also monitored.

For the determination of the mode of inhibition of pentoxifylline, reactions followed the same protocol, using 5-30 μM substrate in the presence of increasing amounts of the inhibitor. The mode of action was determined by plotting the data as Lineweaver-Burk plots, and by fitting all data to the standard competitive inhibition equation with GraFit software [49].

A range of AfChiB1 point mutants were used to assess effects on inhibition—the construction, purification, and kinetic analysis of these mutants have been reported previously [18].

PDE, Lysozyme, Cellulase, and Mammalian Chitinase Enzymology

Commercially available cellulase from *A. niger* (Sigma: C-1184) was assayed using the fluorogenic substrate 4-methylumbelliferyl-β-D-cellobioside (Sigma: M-6018). In a final volume of 50 μl, 5 nM of enzyme was incubated with 20 μM substrate in McIlvain buffer, containing 0.1 mg/ml BSA, for 30 min at 37°C in the presence of different concentration of inhibitors. After the addition of 25 μl of 3 M glycine-NaOH (pH 10.3), the fluorescence of the liberated 4MU was quantified using a fluorescence reader with parameters as for the AfChiB1 experiments. Measurements were performed in triplicate. Production of 4MU was linear with time for the incubation period used, and less than 10% of available substrate was hydrolyzed.

Phosphodiesterase 4A (PDE4A) was assayed using an Sf9-expressed GST-fusion, and activity was monitored by hydrolysis of [^{3}H]cAMP to [^{3}H]AMP using the PDE-SPA kit from Amersham Pharmacia Biotech, as described previously [50]. The assay reaction contained 100 nM [^{3}H]cAMP (1 μCi/ml) in solution containing 20 mM HEPES (pH 7.5), 10 mM $MgCl_2$, 100 mM EDTA, 100mM KCl, and 2 μl of test compound in DMSO at 30°C. The reaction was initiated by addition of enzyme and run for 10 min. The potency of inhibitors (IC_{50}) was determined from a dose-response curve. Experiments were performed with n = 6.

Lysozyme was assayed using the EnzCheck Lysozyme kit from Molecular Probes, as described by the manufacturer. Chicken egg white lysozyme and its substrate, fluorescein-labeled *Micrococcus lysodeikyius* cell wall (DQ lysozyme substrate) were used to determine compound inhibition. Briefly, 6.25 U of lysozyme were incubated with 25 μg of DQ substrate with or without various concentrations of inhibitor in a total volume of 100 μl at 37°C for 30 min. The fluorescence was determined using excitation and emission wavelengths of 360 and 460 nm, respectively. The IC_{50} was determined from a dose-response curve. Experiments were performed in triplicate.

Gene sequences for the human chitotriosidase and AMCase are known [51, 27]. cDNAs encoding human chitotriosidase and human AMCase were generated from total human lung RNA using RT-PCR and primers based on the published sequence (primer pairs: 5′-gcc accatggtgcggtctgtggcctgggcaggtttc-3′ and 5′-tcaattccaggtgcagc atttgcaggagttgctg-3′ for chitotriosidase: 5′-gccaccatgacaaagctt attctcctcacaggtcttg-3′ and 5′-ttatgcccagttgcagcaatcacagctggtgt cgaag-3′ for AMCase), then subcloned into p3xFLAG-CMV-13 vector (Sigma). The vector encodes three adjacent FLAG epitopes downstream of the cloning region. Plasmids encoding FLAG-tagged chitotriosidase and hAMCase were then transiently transfected into HEK 293 cells and supernatants harvested 3 or 6 d after transfection. FLAG-tagged expressing proteins were purified over an anti-FLAG M2 gel affinity column and eluted with a 3XFLAG peptide according to the manufacturer's instructions. Inhibitor potencies were determined for the purified proteins using the chitinase assay similar to the one described above. Briefly, the assay consisted of fluorogenic substrate 4MU-$GlcNAc_2$ (Sigma) at a final concentration of 22 μM, along with 1 nM of enzyme in a final volume of 100 μl. The fluorescence was read using excitation and emission wavelengths of 355 and 460 nm, respectively. The buffers were the same as described above for fungal chitinase, and the reaction was carried out at 30°C for 30 min.

Acknowledgments

We thank Gregg Masters, Gloria Wolfe, John Mudgett, and Gene Porter for human chitinase protein and assay support. This work was supported by a Wellcome Trust Senior Research Fellowship, the EMBO Young Investigator program (both to D.v.A.), and the European Union FP6 STREP Fungwall program.

Received: April 20, 2005
Revised: June 10, 2005
Accepted: July 12, 2005
Published: September 23, 2005

References

1. Coutinho, P.M., and Henrissat, B. (1999). (http://afmb.cnrs-mrs.fr/CAZY).
2. Kuranda, M.J., and Robbins, P.W. (1991). Chitinase is required for cell separation during growth of *Saccharomyces cerevisiae*. J. Biol. Chem. *266*, 19758–19767.
3. Takaya, N., Yamazaki, D., Horiuchi, H., Ohta, A., and Takagi, M.

(1998). Cloning and characterisation of a chitinase-encoding gene chiA from *Aspergillus nidulans*, disruption of which decreases germination frequency and hyphal growth. Biosci. Biotechnol. Biochem. *62*, 60–65.
4. Sakuda, S. (1996). Studies on the chitinase inhibitors, allosamidins. In Chitin Enzymology, Vol. 2. (Ancona, Italy: Atec Edizioni), pp. 203–212.
5. Arnold, K., Brydon, L.J., Chappell, L.H., and Gooday, G.W. (1993). Chitinolytic activities in heligmosomoides-polygyrus and their role in egg hatching. Mol. Biochem. Parasitol. *58*, 317–323.
6. Vinetz, J.M., Valenzuela, J.G., Specht, C.A., Aravind, L., Langer, R.C., Ribeiro, J.M.C., and Kaslow, D.C. (2000). Chitinases of the avian malaria parasite *Plasmodium gallinaceum*, a class of enzymes necessary for parasite invasion of the mosquito midgut. J. Biol. Chem. *275*, 10331–10341.
7. Tsai, Y.-L., Hayward, R.E., Langer, R.C., Fidock, D.A., and Vinetz, J.M. (2001). Disruption of *Plasmodium falciparum* chitinase markedly impairs parasite invasion of mosuito midgut. Infect. Immun. *69*, 4048–4054.
8. Sakuda, S., Isogai, A., Matsumoto, S., Suzuki, A., and Koseki, K. (1986). The structure of allosamidin, a novel insect chitinase inhibitor produced by *Streptomyces* sp. Tetrahedron Lett. *27*, 2475–2478.
9. Cohen, E. (1993). Chitin synthesis and degradation as targets for pesticide action. Arch. Insect Biochem. Physiol. *22*, 245–261.
10. Shiomi, K., Arai, N., Iwai, Y., Turberg, A., Koelbl, H., and Omura, S. (2000). Structure of argifin, a new chitinase inhibitor produced by *Gliocladium* sp. Tetrahedron Lett. *41*, 2141–2143.
11. Arai, N., Shiomi, K., Yamaguchi, Y., Masuma, R., Iwai, Y., Turberg, A., Koelbl, H., and Omura, S. (2000). Argadin, a new chitinase inhibitor, produced by *Clonostachys* sp. FO-7314. Chem. Pharm. Bull. (Tokyo) *48*, 1442–1446.
12. Zhu, Z., Zheng, T., Homer, R.J., Kim, Y.K., Chen, N.Y., Cohn, L., Hamid, Q., and Elias, J.A. (2004). Acidic mammalian chitinase in asthmatic Th2 inflammation and IL-13 pathway activation. Science *304*, 1678–1682.
13. Terwisscha van Scheltinga, A.C., Kalk, K.H., Beintema, J.J., and Dijkstra, B.W. (1994). Crystal structures of hevamine, a plant defense protein with chitinase and lysozyme activity, and its complex with an inhibitor. Structure *2*, 1181–1189.
14. Perrakis, A., Tews, I., Dauter, Z., Oppenheim, A.B., Chet, I., Wilson, K.S., and Vorgias, C.E. (1994). Crystal structure of a bacterial chitinase at 2.3 Å resolution. Structure *2*, 1169–1180.
15. van Aalten, D.M.F., Komander, D., Synstad, B., Gåseidnes, S., Peter, M.G., and Eijsink, V.G.H. (2001). Structural insights into the catalytic mechanism of a family 18 exo-chitinase. Proc. Natl. Acad. Sci. USA *98*, 8979–8984.
16. Hollis, T., Mozingo, A.F., Bortone, K., Ernst, S., Cox, R., and Robertus, J.D. (2000). The X-ray structure of a chitinase from the pathogenic fungus *Coccidioides immitis*. Protein Sci. *9*, 544–551.
17. Fusetti, F., von Moeller, H., Houston, D., Rozeboom, H.J., Dijkstra, B.W., Boot, R.G., Aerts, J.M.F.G., and van Aalten, D.M.F. (2002). Structure of human chitotriosidase: implications for specific inhibitor design and function of mammalian chitinase-like lectins. J. Biol. Chem. *277*, 25537–25544.
18. Rao, F.V., Houston, D.R., Boot, R.G., Aerts, J.M.F.G., Hodkinson, M., Adams, D.J., Shiomi, K., Omura, S., and van Aalten, D.M.F. (2005). Specificity and affinity of natural product cyclopentapeptide inhibitors against *Aspergillus fumigatus*, human and bacterial chitinases. Chem. Biol. *12*, 65–76.
19. Tews, I., Terwisscha van Scheltinga, A.C., Perrakis, A., Wilson, K.S., and Dijkstra, B.W. (1997). Substrate-assisted catalysis unifies two families of chitinolytic enzymes. J. Am. Chem. Soc. *119*, 7954–7959.
20. Papanikolau, Y., Tavlas, G., Vorgias, C.E., and Petratos, K. (2003). De novo purification scheme and crystallization conditions yield high-resolution structures of chitinase A and its complex with the inhibitor allosamidin. Acta Crystallogr. D Biol. Crystallogr. *59*, 400–403.
21. Bortone, K., Monzingo, A.F., Ernst, S., and Robertus, J.D. (2002). The structure of an allosamidin complex with the *Coccidioides immitis* chitinase defines a role for a second acid residue in substrate-assisted mechanism. J. Mol. Biol. *320*, 293–302.
22. Izumida, H., Imamura, N., and Sano, H. (1996). A novel chitinase inhibitor from a marine bacterium *Pseudomonas* sp. J. Antibiot. (Tokyo) *49*, 76–80.
23. Houston, D.R., Shiomi, K., Arai, N., Omura, S., Peter, M.G., Turberg, A., Synstad, B., Eijsink, V.G.H., and van Aalten, D.M.F. (2002). High-resolution structures of a chitinase complexed with natural product cyclopentapeptide inhibitors: mimicry of carbohydrate substrate. Proc. Natl. Acad. Sci. USA *99*, 9127–9132.
24. Houston, D.R., Eggleston, I., Synstad, B., Eijsink, V.G.H., and van Aalten, D.M.F. (2002). The cyclic dipeptide CI-4 inhibits family 18 chitinases by structural mimicry of a reaction intermediate. Biochem. J. *368*, 23–27.
25. Houston, D.R., Synstad, B., Eijsink, V.G.H., Stark, M.J.R., Eggleston, I.M., and van Aalten, D.M.F. (2004). Structure-based exploration of cyclic dipeptide chitinase inhibitors. J. Med. Chem. *47*, 5713–5720.
26. Hollak, C.E.M., van Weely, S., van Oers, M.H.J., and Aerts, J.M.F.G. (1994). Marked elevation of plasma chitotriosidase activity: a novel hallmark of Gaucher disease. J. Clin. Invest. *93*, 1288–1292.
27. Boot, R.G., Blommaart, E.F.C., Swart, E., Ghauharali-van der Vlugt, K., Bijl, N., Moe, C., Place, A., and Aerts, J.M. (2001). Identification of a novel acidic mammalian chitinase distinct from chitotriosidase. J. Biol. Chem. *276*, 6770–6778.
28. Bergstrand, H. (1980). Eur. J. Respir. Dis. Suppl. *109*, 37–44.
29. Meskini, N., Nemoz, G., Okyayuzbaklouti, I., Lagarde, M., and Prigent, A.F. (1994). Phosphodiesterase inhibitory profile of some related xanthine derivatives pharmacologically active on the peripheral microcirculation. Biochem. Pharmacol. *47*, 781–788.
30. Fredholm, B.B., and Persson, C.G.A. (1982). Xanthine derivatives as adenosine receptor antagonists. Eur. J. Pharmacol. *81*, 673–676.
31. Ito, K., Lim, S., Caramori, G., Cosio, B., Chung, K.F., Adcock, I.M., and Barnes, P.J. (2002). A molecular mechanism of action of theophylline: induction of histone deacetylase activity to decrease inflammatory gene expression. Proc. Natl. Acad. Sci. USA *99*, 8921–8926.
32. Rabe, K.F., Magnussen, H., and Dent, G. (1995). Theophylline and selective PDE inhibitors as bronchodilators and smooth-muscle relaxants. Eur. Respir. J. *8*, 637–642.
33. Koga, D., Isogai, A., Sakuda, S., Matsumoto, S., Suzuki, A., Kimura, S., and Ide, A. (1987). Specific inhibition of *Bombyx-mori* chitinase by allosamidin. Agric. Biol. Chem. *51*, 471–476.
34. van Aalten, D.M.F., Synstad, B., Brurberg, M.B., Hough, E., Riise, B.W., Eijsink, V.G.H., and Wierenga, R.K. (2000). Structure of a two-domain chitotriosidase from *Serratia marcescens* at 1.9 Å resolution. Proc. Natl. Acad. Sci. USA *97*, 5842–5847.
35. Rao, F.V., Houston, D.R., Boot, R.G., Aerts, J.M.F.G., Sakuda, S., and van Aalten, D.M.F. (2003). Crystal structures of allosamidin derivatives in complex with human macrophage chitinase. J. Biol. Chem. *278*, 20110–20116.
36. Davies, G.J., Wilson, K.S., and Henrissat, B. (1997). Nomenclature for sugar-binding subsites in glycosyl hydrolases. Biochem. J. *321*, 557–559.
37. Papanikolau, Y., Prag, G., Tavlas, G., Vorgias, C.E., Oppenheim, A.B., and Petratos, K. (2001). High resolution structural analyses of mutant chitinase A complexes with substrates provide new insight into the mechanism of catalysis. Biochemistry *40*, 11338–11343.
38. Huai, Q., Liu, Y.D., Francis, S.H., Corbin, J.D., and Ke, H.M. (2004). Crystal structures of phosphodiesterases 4 and 5 in complex with inhibitor 3-isobutyl-1-methylxanthine suggest a conformation determinant of inhibitor selectivity. J. Biol. Chem. *279*, 13095–13101.
39. Scapin, G., Patel, S.B., Chung, C., Varnerin, J.P., Edmondson, S.D., Mastracchio, A., Parmee, E.R., Singh, S.B., Becker, J.W., Van der Ploeg, L.H.T., et al. (2004). Crystal structure of human phosphodiesterase 3B: atomic basis for substrate and inhibitor specificity. Biochemistry *43*, 6091–6100.
40. Donnelly, L.E., and Barnes, P.J. (2004). Acidic mammalian chi-

tinase: a potential target for asthma therapy. Trends Pharmacol. Sci. *25*, 509–511.
41. Weinberger, M., and Hendeles, L. (1996). Drug therapy: theophylline in asthma. N. Engl. J. Med. *334*, 1380–1388.
42. Entzian, P., Bitter-Suermann, S., Burdon, D., Ernst, M., Schlaak, M., and Zabel, P. (1998). Differences in the anti-inflammatory effects of theophylline and pentoxifylline: important for the development of asthma therapy? Allergy *53*, 749–754.
43. Abdel-Salam, O.M.E., Baiuomy, A.R., El-Shenawy, S.M., and Arbid, M.S. (2003). The anti-inflammatory effects of the phosphodiesterase inhibitor pentoxifylline in the rat. Pharmacol. Res. *47*, 331–340.
44. Fleming, C.M., He, H.Z., Ciota, A., Perkins, D., and Finn, P.W. (2001). Administration of pentoxifylline during allergen sensitization dissociates pulmonary allergic inflammation from airway hyperresponsiveness. J. Immunol. *167*, 1703–1711.
45. Otwinowski, Z., and Minor, W. (1997). Processing of X-ray diffraction data collected in oscillation mode. Methods Enzymol. *276*, 307–326.
46. Brunger, A.T., Adams, P.D., Clore, G.M., Gros, P., Grosse-Kunstleve, R.W., Jiang, J.-S., Kuszewski, J., Nilges, M., Pannu, N.S., Read, R.J., et al. (1998). Crystallography and NMR system: a new software system for macromolecular structure determination. Acta Crystallogr. D Biol. Crystallogr. *54*, 905–921.
47. Jones, T.A., Zou, J.Y., Cowan, S.W., and Kjeldgaard, M. (1991). Improved methods for building protein models in electron density maps and the location of errors in these models. Acta Crystallogr. A *47*, 110–119.
48. Schuettelkopf, A.W., and van Aalten, D.M.F. (2004). PRODRG: a tool for high-throughput crystallography of. Acta Crystallogr. D Biol. Crystallogr. *60*, 1355–1363.
49. Leatherbarrow, R.J. (2001). GraFit Version *5* (Horley, UK: Erithacus Software Ltd.).
50. Percival, M.D., Yeh, B., and Falgueyret, J.P. (1997). Zinc dependent activation of cAMP-specific phosphodiesterase (PDE4A). Biochem. Biophys. Res. Commun. *241*, 175–180.
51. Boot, R.G., Renkema, G.H., Strijland, A., van Zonneveld, A.J., and Aerts, J.M.F.G. (1995). Cloning of a cDNA-encoding chitotriosidase, a human chitinase produced by macrophages. J. Biol. Chem. *270*, 26252–26256.
52. Vriend, G. (1990). WHAT IF: a molecular modeling and drug design program. J. Mol. Graph. *8*, 52–56.

Accession Numbers

The coordinates and structure factors have been deposited with the PDB: entries 2A3A (AfChiB1 + theophylline), 2A3B (AfChiB1 + caffeine), 2A3C (AfChiB1) + pentoxifylline), and 2A3E (AfChiB1 + allosamidin).